Perceptual Quality Assessment for 3D Triangle Mesh Based on Curvature

Lu Dong, Yuming Fang, Weisi Lin, *Senior Member, IEEE*, and Hock Soon Seah

***Abstract*—Triangle meshes are used in representation of 3D geometric models, and they are subject to various visual distortions during geometrical processing and transmission. In this study, we propose a novel objective quality assessment method for 3D meshes based on curvature information; according to characteristics of the human visual system (HVS), two new components including visual masking and saturation effect are designed for the proposed method. Besides, inspired by the fact that the HVS is sensitive to structural information, we compute the structure distortion of 3D meshes. We test the performance of the proposed method on three publicly available databases of 3D mesh quality evaluation. We rotate among these databases for parameter determination to demonstrate the robustness of the proposed scheme. Experimental results demonstrate that the proposed method can predict consistent results in terms of correlation to the subjective scores across the databases.**

***Index Terms*—Curvature, human visual system, quality assessment, saturation effect, structure distortion, visual masking.**

I. Introduction

With the advance of computer hardware and software, a large number of visual contents have been created and viewed in various applications such as entertainment (e.g. game, movie), education, and medical fields. In this work, we investigate issues on quality evaluation for 3D geometric models that are mostly represented by triangle meshes. In various geometry processing operations, such as compression and watermarking, visual distortions are likely to be introduced into the original 3D meshes. Visual quality assessment of 3D meshes is critical since such a criterion can be used in design and optimization of graphic algorithms and systems.

Manuscript received November 26, 2014; revised June 05, 2015; accepted September 18, 2015. Date of publication September 29, 2015; date of current version November 13, 2015. This work was supported in part by the Singapore MoE Tier 1 Project M4011379 RG141/14, by the National NSF of China under Grant 61571212, Grant 20142BAB217011, and Grant 20151BDH80003, and by the Scientific Research Foundation for the Returned Overseas Chinese Scholars, State Education Ministry, China. The associate editor coordinating the review of this manuscript and approving it for publication was Prof. Maria Martini. *(Corresponding author: Yuming Fang.)*

L. Dong, W. Lin, and H. S. Seah are with the School of Computer Engineering, Nanyang Technological University, Singapore 639798 (e-mail: s090059@e.ntu.edu.sg; WSLin@ntu.edu.sg; ashsseah@ntu.edu.sg).

Y. Fang is with the School of Information Technology, Jiangxi University of Finance and Economics, Nanchang 330032, China (e-mail: FA0001NG@e.ntu.edu.sg).

Color versions of one or more of the figures in this paper are available online at http://ieeexplore.ieee.org.

Digital Object Identifier 10.1109/TMM.2015.2484221

In this work, we focus on quality evaluation of 3D triangle meshes based on curvature information, with formulation on perceptual effects with visual masking, saturation and structure. Curvature describes visual characteristics of 3D surfaces and has been applied in existing quality evaluation methods [1]–[5]. In these methods, the quality of a distorted model is measured through perceptual comparison in curvature between vertices of a reference model and the distorted model. Distorted models studied in this work are with the same connectivity as the corresponding reference models, similar to some existing studies [1], [6]–[8].

Since the Human Visual System (HVS) is the ultimate evaluator of the majority of (if not all) produced 3D triangle meshes, an objective quality assessment method which correlates well with human perception needs to be designed. The HVS has developed unique characteristics in processing and understanding of visual information. Existing studies have demonstrated that incorporating perceptual properties of the HVS will benefit various 3D multimedia applications [9], [10], such as 3D model transmission [11], 3D model watermarking [12], 3D mesh simplification [13], and perceptual 3D rendering [14], [15]. The characteristics of the HVS have been considered in existing quality metrics for 3D meshes [1]–[5], [8]. Given a high-quality reference mesh and a distorted mesh, features of the surface, such as curvature [1] and dihedral angle [8], are calculated for each vertex/face of the meshes. The differences between the features of these two meshes are computed and modulated by perceptual components such as visual masking component [3]–[5], [8] and the saturation component [3] to predict the perceived differences by human observers. For the distorted mesh, a final quality score is obtained by integrating the perceived feature differences on the surfaces.

Visual masking refers to the decrease of visibility of visual signals with the presence of background signals [16]. In the context of 3D mesh quality evaluation, visual masking indicates that distortions are less visible on rough regions. Visual masking has been applied in 3D mesh quality evaluation in existing methods [3]–[5], [8]. A roughness measure is computed from surface features (curvature, dihedral angle, etc.), and objective distortions are modulated by the roughness measure. The roughness measure used in [3] is the Laplacian of Gaussian curvature, which is calculated in 1-ring (nearest) neighbors of a center vertex. Roughness distortions are measured between a reference and a distorted model, and the local roughness distortion is modulated by a power function of the roughness. The smoothness measure defined in [8] is the dihedral angle between two adjacent triangles. The local difference in smoothness is modulated by an exponential function of the smoothness. As a result, the

objective distortion is amplified to a larger extent in faces with larger dihedral angles. The roughness measure defined in [5] is the Laplacian of the mean curvatures in 1-ring neighborhood of a vertex. In [5], the local perceptual distance between the curvature tensors is computed as a product of the roughness and the objective tensor difference.

For the visual masking components introduced above, the roughness measures are computed from the nearest neighbors of a vertex or face. The variation in a small neighborhood is usually not significant, and thus it may be inaccurate to determine whether a region is rough or not solely based on the statistics extracted from a small neighborhood. The details will be analyzed in Section III-C. To overcome these problems, the roughness measure used in the visual masking module is calculated as the Gaussian-weighted average of mean curvature in a local neighborhood. Although the use of Gaussian-weighted averaged curvature has been introduced in [1] for computation of feature distortion, it has not been used to modulate objective distortion in a visual masking component. Further, inspired by the fact that edges and rough regions exhibit different levels of masking effect [12], we assign different masking weights to rough regions and edges in the visual masking computation. The details of the component will be analyzed in Section III-C.

Saturation effect in visual quality evaluation was first introduced by Lambrecht *et al.* [17]; this effect indicates that the sensitivity of the HVS to distortions decreases at high distortion levels. That is, when the distortion level is high, it would be difficult for human observers to perceive further increase in distortion level. Saturation effect has been considered in various quality evaluation methods for natural images and videos, such as [18]–[20]. Saturation effect has first been considered in quality evaluation of 3D meshes in [3], by limiting the calculated roughness to the range of $[Th_l, Th_h]$. In the metric [3], the distortion of a distorted mesh is computed as the difference of global roughness between the distorted mesh and a reference mesh. Therefore, by clamping the roughness to the range of $[Th_l, Th_h]$, the upper threshold of the computed distortion level is set as $Th_h - Th_l$. However, setting an upper threshold of distortion cannot reflect the decrease in sensitivity to distortion at high distortion levels. In this study, we model the saturation effect with an exponential function to reflect the decrease in sensitivity to perceived distortion at high distortion levels. The details of the saturation module will be analyzed in Section III-D.

Besides the visual masking and saturation modules, we also propose a method to compute the structure similarity between a distorted model and a reference one. According to existing studies in quality evaluation of natural images/videos [21], the HVS is sensitive to structural information. To measure structural distortion of a distorted 3D mesh, we detect strong edges and measure the similarity of the edge strength between the distorted and reference meshes.

The main contributions of this work include three aspects. First, we design a new module for visual masking in quality assessment of 3D meshes. A roughness measure is calculated as the Gaussian-weighted average of mean curvature in a neighborhood and a masking function on the roughness measure is employed to decrease perceived distortion at rough regions. Second, we design a new component in the proposed method to account for the saturation effect in the HVS. Different from the existing saturation component [3], the proposed component is able to simulate the decrease in sensitivity of the HVS to distortions at high distortion levels. Third, we compute the structure distortion of 3D meshes, to evaluate the distortion imposed on the structural information of meshes.

We conduct experiments to demonstrate the performance of the proposed method on three publicly available databases: the LIRIS/EPFL general-purpose database [1], the LIRIS masking database [12], and the UWB compression database [8]. Experimental results demonstrate that the proposed method yields consistent results across these databases in alignment with human perception.

II. Related Work

To predict human judgement on quality of 3D triangle meshes, model-based perceptual quality assessment methods [1]–[8], [22], [23] have been designed. Model-based methods try to extract features from 3D geometrical models, and predict the quality of 3D models based on the difference in features between reference and distorted models. Detailed reviews of model-based perceptual metrics can be referred to [24], [25].

According to existing studies, the classical geometric distances, like Hausdorff distance (HD) and Root Mean Square Error (RMS) do not correlate well with human visual perception [25]. Thus different features have been explored in existing works. Karni and Gotsman [6] argued that a geometrical Laplacian operator captures visual properties of surfaces, e.g. smoothness. They formulated the difference between a reference model and a distorted model as the average of differences in both vertex coordinates and Laplacian values between corresponding vertices in the models. Later, Sorkine *et al.* [22] improved the method [6] by giving a greater weight to the Laplacian values in the distortion measure. Bian *et al.* [7] proposed a quality assessment metric based on the level of energy which causes the deformation to the reference model, i.e. the strain energy. Corsini *et al.* [23] proposed a method based on the roughness, which is a measure of the variation in surface vertices. Two formulations of roughness measure were derived, and quality of a distorted model was measured based on the per-vertex difference in roughness between the distorted and reference models. Váša and Rus [8] derived a quality assessment metric by computing the differences in oriented dihedral angles between triangles in 3D models.

In this study, we focus on investigating quality evaluation for 3D meshes based on curvature information, according to the fact that the HVS is sensitive to curvature changes [26]. In fact, curvature information has been successfully used in several existing methods [1]–[5]. Lavoué *et al.* [1] proposed a method based on the computation of difference in mean curvature between vertices of the reference and distorted models. Lavoué [2] later extended the work [1] to handle changed connectivity of distorted models. Wang *et al.* [3] computed the Laplacian of discrete Gaussian curvature for each vertex on a model, and derived a global roughness measure by adding the Laplacian values. The quality of a model is measured through perceptual comparison between the global roughness measure of the model and that of the reference model. The studies [4], [5] employ both curvature

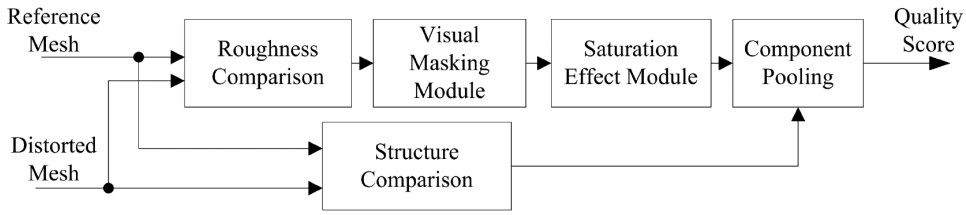

Fig. 1. Pipeline of the proposed 3D mesh quality assessment method.

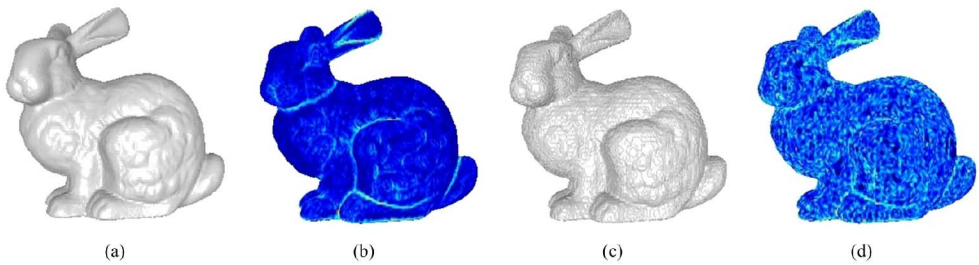

Fig. 2. Mean curvature describes the visual characteristics of 3D models. (a) Reference bunny model. (b) Mean curvature map of the object in (a). (c) Distorted model after quantization of coordinates. (d) Mean curvature map of the object in (c).

amplitude and principal curvature directions for quality evaluation of 3D meshes.

III. The Proposed Method

A. Overview

The pipeline of the proposed method is shown in Fig. 1. The proposed method relies on both roughness comparison and structure comparison. Given a reference model and a distorted model, the proposed method calculates the mean curvature value (κ_{mean}) for each vertex in the models, and then computes the roughness of the vertex as a Gaussian-weighted average of mean curvature values ($\tilde{\kappa}_{\text{mean}}$) in the neighborhood of the vertex. After that, the proposed method computes the difference in roughness ($\tilde{\kappa}_{\text{mean}}$) between each pair of vertices from these two models. The computed roughness difference (variation) is then modulated by visual masking and saturation components. Additionally, the method computes the structure similarity between these two models. Finally, a quality score of the distorted mesh is derived through pooling the roughness similarity score and the structure similarity score. In image quality evaluation methods, pooling refers to the process integrating the quality (distortion) values obtained from different components into a final quality (distortion) score.

B. Computation of Roughness Difference

Intuitively, curvature describes the deviation amount of a surface from being flat. Discrete curvature has been considered in several existing methods of 3D mesh quality assessment [1]–[5], due to its ability to describe the visual characteristics of 3D meshes [1]. Fig. 2 illustrates two mean curvature maps for a reference Bunny model, and a distorted Bunny model. The model in Fig. 2(c) is created by applying coordinate quantization on the original model in Fig. 2(a). In Fig. 2(b) and (d), warmer colors indicate higher mean curvature values. After the quantization, the surface of the Bunny becomes rougher from (a) to (c), and the mean curvature map becomes noisier from (b) to (d). We can see that mean curvature information is variant to surface roughness.

3D mesh is a piecewise-linear approximation of continuous surface, and there are various definitions of curvature tensor on a mesh [27]. Similar as in [2], we adopt the method proposed by Alliez *et al.* [28], to estimate the curvature tensor at each vertex of the mesh. The method estimates the curvature tensor on a geodesic disk neighborhood around each vertex, and yields stable results independent of the sampling density of the model [2]. The maximum curvature $\kappa_{\max}$ and the minimum curvature $\kappa_{\min}$ are calculated from the curvature tensor. The mean curvature κ_{mean} is computed as $(\kappa_{\max} + \kappa_{\min})/2$.

For each vertex, a roughness measure is computed as the Gaussian-weighted average of mean curvature ($\tilde{\kappa}_{\text{mean}}$) in a spherical neighborhood around the vertex [2]. The Gaussian-weighted average of mean curvature $\tilde{\kappa}_{\text{mean}}(v)$ of vertex v is computed as

$$\tilde{\kappa}_{\text{mean}}(v) = \frac{\sum_{v_m \in \mathcal{S}(v)} \exp\left(-2||v_m - v||^2/\gamma^2\right) \cdot \kappa_{\text{mean}}(v_m)}{\sum_{v_m \in \mathcal{S}(v)} \exp\left(-2||v_m - v||^2/\gamma^2\right)} \tag{1}$$

where v_m is a vertex in the spherical neighborhood $\mathcal{S}$ of v; $\kappa_{\text{mean}}(v_m)$ is the mean curvature value of the vertex; γ is the radius of the neighborhood; $||v_m - v||$ is the Euclidean distance between vertex v_m and v. Here we compute the roughness measure in a spherical neighborhood instead of a 1-ring neighborhood for the reason that curvature computed in a larger neighborhood is a better indicator of surface roughness, which will be demonstrated with an example in Fig. 4. The difference in roughness between a vertex in a distorted model and the corresponding vertex in a reference model is calculated as follows:

$$D_R(v_i^r, v_j^d) = \frac{|\tilde{\kappa}_{\text{mean}}(v_i^r) - \tilde{\kappa}_{\text{mean}}(v_j^d)|}{C_1} \tag{2}$$

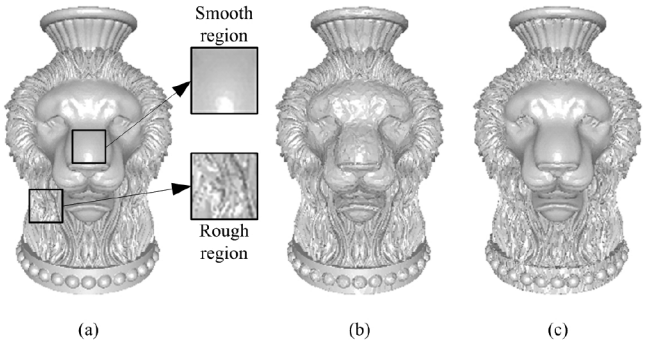

Fig. 3. Example of visual masking effect. (a) Original LionVase model. (b) Distorted mesh created by adding medium-level noise in smooth regions. (c) Distorted mesh created by adding high-level noise in rough regions.

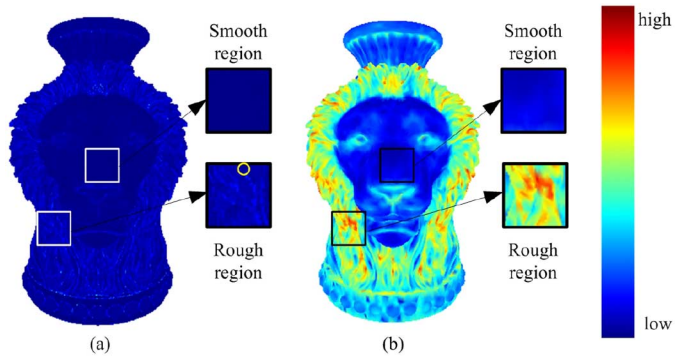

Fig. 4. Mean curvature maps for the LionVase model (a) calculated in 1-ring neighborhood of each vertex and (b) calculated in a larger neighborhood as (1).

where v_j^d is a vertex in the distorted model M_d; v_i^r is the corresponding vertex in the reference model M_r; $\tilde{\kappa}_{\text{mean}}(v_i^r)$ and $\tilde{\kappa}_{\text{mean}}(v_j^d)$ is the roughness of v_i^r and v_j^d, respectively; $|\cdot|$ computes the absolute value; C_1 is a normalizing constant, which corresponds to the dynamic range of the roughness value.

C. Visual Masking Formulation

Visual masking is an important characteristic of the HVS. In the context of quality assessment of 3D meshes, visual masking indicates that artifacts become less visible on rough regions to human observers. Fig. 3 illustrates an example of visual masking effect. Fig. 3(a) is the original LionVase model and two examples of smooth region and rough region in this model are highlighted. Fig. 3(b) is a distorted model created by adding medium-level noise in smooth regions, while Fig. 3(c) is a distorted model created by adding high-level noise in rough regions. Although the objective level of distortion in Fig. 3(c) (high-level noise) is higher than that in Fig. 3(b) (medium-level noise), the perceived quality in Fig. 3(c) is better, since noise in the mane of the Lion is less annoying than noise in smooth regions of the face.

To take the visual masking effect into account for quality assessment, we try to mask the distortion in rough regions. Existing methods [3]–[5], [8] calculate the roughness measure based on statistics extracted from a 1-ring neighborhood of a vertex or triangle. However, there are a large number of vertices in a typical 3D model and thus vertex features, such as geometry coordinate, curvature, or dihedral angle, do not vary greatly in the 1-ring neighborhood. Due to the small variation, it is difficult to determine whether a local region is rough or not by the variation. Fig. 4(a) shows the mean curvature map for the LionVase model, calculated in 1-ring neighborhood of each vertex, and warmer colors indicate higher mean curvature values. As can be observed from Fig. 4(a), although the vertices in the highlighted rough region exhibit higher curvature values than the vertices in the highlighted smooth region, vertices are with low curvature values (dark blue colors). Some vertices in the rough region (e.g. the pixels highlighted with the circle in the rough region) have similar curvature values as vertices in the smooth region, and the masking potential of these vertices will be under-estimated.

As mentioned in Section III-B, the roughness measure is obtained by computing the average curvature ($\tilde{\kappa}_{\text{mean}}$) of vertices in a large spherical neighborhood of each vertex. The radius is set to 0.2% of the maximum length of the bounding box of the model. A proper choice of radius also depends on the display resolution, viewing distance and sampling density at different parts of each model. For example, the local regions of the mane in the LionVase model from Fig. 3(a) are considered as rough from a large viewing distance, but they may be considered as smooth if the viewing distance is sufficiently small to view every vertex clearly. In this work, the models are shown on a 19-inch LCD monitor with display resolution at 1440×900 pixels, and we set the radius to 0.2% empirically. An example of the curvature map is illustrated in Fig. 4(b). From this figure, we can see that the vertices in the rough regions are with high values (orange colors), while vertices in the smooth regions are with lower values (dark blue colors). Compared with Fig. 4(a), rough region can be better distinguished from smooth regions in Fig. 4(b).

To mask the roughness variation in rough regions, we multiply the roughness variation $D_R(v_i^r, v_j^d)$ in (2) by a masking function. The visual masking tuned roughness difference $D_{\text{masking}}(v_i^r, v_j^d)$ is calculated as follows:

$$D_{\text{masking}}(v_i^r, v_j^d) = D_R(v_i^r, v_j^d) \cdot \exp\left(-\frac{\tilde{\kappa}_{\text{mean}}(v_i^r)^2}{2\sigma^2}\right) \tag{3}$$

where σ is a parameter of the Gaussian kernel. With the function, the roughness variation in smooth regions will not be modified significantly (masking coefficient is near the value "1"), to account for the weak masking ability of these vertices. The computed roughness variation in rough regions will be reduced to a larger extent (masking coefficient is significantly smaller than the value "1"), to account for the strong masking ability of these vertices.

According to existing studies in quality assessment of 3D meshes [12] and natural images/videos [29], rough regions in 3D meshes (or textural regions in natural images) exhibit stronger visual masking effect than edges. Due to the entropy masking effect [30], the visibility to a visual signal decreases when the masking signal is unfamiliar or uncertain to human eyes. Rough regions in 3D meshes are less predictable than edges, and thus have stronger visual masking effect. Therefore,

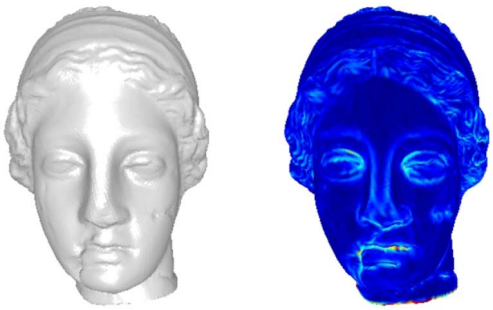

(a) (b)

Fig. 5. Maximum curvature map of the Venus model. (a) Reference Venus model. (b) Maximum curvature map of the Venus model.

to take the entropy masking property into account, we assign different visual masking weights to rough regions and edges in the proposed visual masking module.

Since sharp edges are with high maximum curvature (κ_{max}) values, we detect vertices with high maximum curvature values. An example of the maximum curvature map of the Venus model is illustrated in Fig. 5(b). In this figure, sharp edges are with warmer colors (higher κ_{max} values). In the proposed component, the σ value in (3) is determined by whether a vertex belongs to edges or not

$$\sigma(v_i^r) = \begin{cases} \sigma_o \cdot \omega_r, & \kappa_{\max}(v_i^r) \le T_r \\ \sigma_o \cdot \omega_e, & \kappa_{\max}(v_i^r) > T_r \end{cases} \tag{4}$$

where vertices which satisfy $\kappa_{\max}(v_i^r) > T_r$ are detected as edge vertices, while vertices which satisfy $\kappa_{\max}(v_i^r) \le T_r$ are classified as non-edge vertices. Note that non-edge vertices include both rough vertices and smooth vertices. However, for a smooth vertex, the weighting term, $\exp(-\frac{\tilde{\kappa}_{\text{mean}}(v_i^r)^2}{2\sigma^2})$, in (3) is nearly the value "1" since $\tilde{\kappa}_{\text{mean}}(v_i^r)$ is nearly zero. Therefore, the condition $\kappa_{\max}(v_i^r) \le T_r$ affects only the weighting terms of rough regions. In (4), σ_o is a constant; ω_r is the weight for rough vertices and ω_e is the weight for edge vertices; ω_r is set to be smaller than ω_e so that the masking effect in rough vertices is stronger than edges, since a smaller σ induces a shaper slope in the Gaussian function. σ_o controls the shape of the masking function. When σ_o is small, the masking coefficient decreases rapidly from 1 to 0 as the roughness value increases. When σ_o is large, the masking effect assigned to rough regions is weak. In an extreme case, when σ_o approaches positive infinity, the result is the same as the case without the visual masking module.

With the module, distortions in rough regions will be masked. For the two models in Fig. 3(b) and (c), the roughness differences, and the modulated roughness differences are listed in Table I. As shown in Table I, the roughness difference of Fig. 3(b) is smaller than that of Fig. 3(c). That means the computed distortion level of Fig. 3(b) is lower than that of Fig. 3(c), and that is contradictory to the visual comparison result that (b) has worse visual quality than (c). With the visual masking module, the computed roughness difference of Fig. 3(b) is larger than that of Fig. 3(c) and this result is consistent with the visual comparison result.

TABLE I
ROUGHNESS DIFFERENCE AND MODULATED ROUGHNESS DIFFERENCE OF TWO DISTORTED MODELS

Type	Fig. 3(b)	Fig. 3(c)
Roughness Difference	0.285	0.394
Modulated Roughness Difference	0.138	0.047

D. Saturation Effect Modulation

Saturation effect indicates that sensitivity to perceived distortion decreases at high distortion levels [3], [17], [31]. We provide an example of the saturation effect in Fig. 6. This figure includes four distorted Bunny models created by adding uniform noise of different intensities into the reference model, with the MEPP software [2]. The intensity level is relative to the average distance from vertices to mesh center, and a higher intensity level induces larger distortion in the models. Compared with the reference model in Fig. 2(a), the distorted model in Fig. 6(a) exhibits high visual quality, while the model in Fig. 6(b) exhibits worse visual quality, and noise is visible on the mesh surface. The models in Fig. 6(c) and (d) exhibit bad visual quality, and the perceived noise levels are high in the models. Although the objective difference in distortion levels between the models in Fig. 6(a) and Fig. 6(b) is the same as the difference in distortion levels between the models in Fig. 6(c) and Fig. 6(d), observers are likely to assign significantly different scores to the models in Fig. 6(a) and Fig. 6(b), but to assign similar scores to the models in Fig. 6(c) and Fig. 6(d), since observers are not sensitive to slight differences at very bad quality conditions.

We model the saturation effect by an exponential formula as Fig. 7. The mapped curvature difference D_{sat} is calculated as follows:

$$D_{\text{sat}}(v_i^r, v_j^d) = 1 - \exp\left(\frac{-D_{\text{masking}}(v_i^r, v_j^d)}{\beta}\right) \tag{5}$$

where β is the parameter to control the shape of the saturation function. Fig. 8 illustrates the shapes of the saturation functions with different β. In extreme cases, when β approaches 0, the objective distortion values are all mapped to value "1"; when β approaches positive infinity, the objective distortion values are all mapped to value "0". Thus with the increase of β, the performance increases first but decreases later.

To illustrate how the plot in Fig. 7 simulates the saturation effect, we show four distorted models, M_1, M_2, M_3 and M_4, of a same reference model, as an example. In Fig. 7, $D(M1)$, $D(M2)$, $D(M3)$ and $D(M4)$ denote the roughness difference (distortion level) for distorted models M_1, M_2, M_3 and M_4, respectively, without the saturation module. From this figure, M_3 is with larger distortion level than M_1 (i.e. $D(M3) > D(M1)$). $\Delta D(M_1, M_2)$ is the difference in distortion level between M_1 and M_2; $\Delta D(M_3, M_4)$ is the difference in distortion level between M_3 and M_4; $\Delta D(M_1, M_2) = \Delta D(M_3, M_4)$. $\Delta D_{\text{sat}}(M_1, M_2)$ is the difference in distortion level between M_1 and M_2 with the saturation module; $\Delta D_{\text{sat}}(M_3, M_4)$ is the difference in distortion level between M_3 and M_4 with the saturation module. We can see that $\Delta D_{\text{sat}}(M_3, M_4) < \Delta D_{\text{sat}}(M_1, M_2)$, which means the

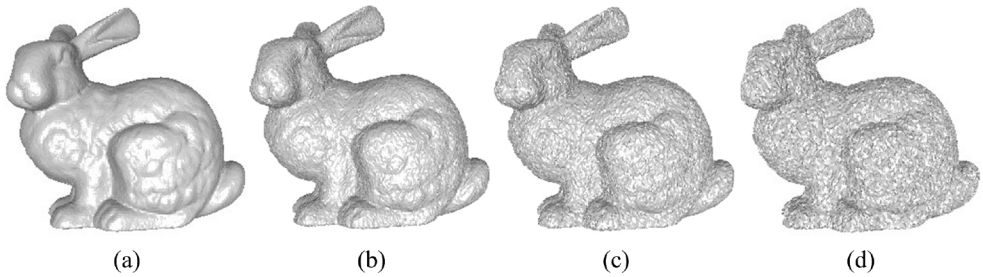

(a) (b) (c) (d)

Fig. 6. Example on saturation effect. Distorted bunny models are created by adding uniform noise with intensity of (a) 0.001, (b) 0.004, (c) 0.007, and (d) 0.010 into the reference bunny model shown in Fig. 2(a).

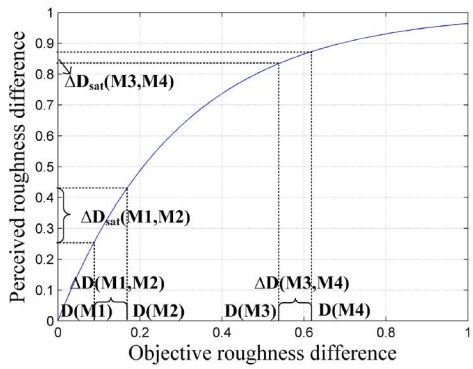

Fig. 7. Saturation effect modulation function.

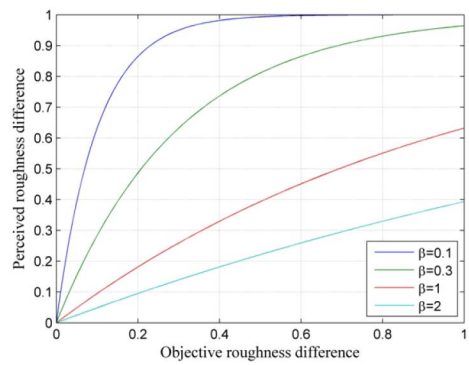

Fig. 8. Shape of the saturation function with different β.

sensitivity to perceived distortion decreases at high distortion levels.

With the saturation module, a perceptual roughness similarity value between a reference model M^r and a distortion model M^d is calculated as

$$S_R(M^r, M^d) = 1 - \frac{1}{|M^r|} \cdot \sum D_{\text{sat}}(v_i^r, v_j^d) \qquad (6)$$

where $|M^r| = |M^d|$ is the total number of vertices in each model.

Note that the output of the roughness comparison and the structure comparison is a value. A distortion map can be extracted as an intermediate result after applying the saturation module. Fig. 9 shows the roughness distortion maps of the Armadillo, Dyno, Venus and RockerArm models. We can see that regions with higher degradation are detected with higher distortion values.

E. Structure Distortion

According to existing studies in quality evaluation of natural images [20], [21], the HVS is sensitive to structural distortion. A typical distortion which degrades the structure of 3D meshes is the smoothing or blurring distortion. The blur of structure is annoying to human observers. Roughness comparison cannot well measure the structural distortion, since the distortion occurs mostly on edges of the meshes, and the roughness does not change greatly for most non-edge vertices. To capture structural distortion of 3D meshes, we detect strong edges of the meshes and compare the similarity between the edge strength of the strong edges in these two meshes. Since sharp edges are with high maximum curvature ($\kappa_{\max}$) values, we detect vertices with high maximum curvature values and include these vertices in computation of structure distortion. To compute the structure similarity, we compute the similarity in $\kappa_{\max}$ values between vertices with high $\kappa_{\max}$ values in the reference model and the corresponding vertices in the distorted model. More specifically, the structure similarity is computed as follows:

$$S_S(M^r, M^d) = \frac{1}{N} \sum_{\kappa_{\max}(v_i^r) > T_r} \frac{2\kappa_{\max}(v_i^r)\kappa_{\max}(v_j^d) + C_2}{\kappa_{\max}^2(v_i^r) + \kappa_{\max}^2(v_j^d) + C_2} \qquad (7)$$

where T_r is a parameter determining which vertices are included in the computation of structure similarity; N is the number of vertices, which satisfy $\kappa_{\max}(v_i^r) > T_r$ in the reference model; C_2 is a small constant to avoid the denominator being zero (e.g. $C_2 = 10^{-5}$).

Fig. 10 shows a noise distorted model (b) and a smoothing distorted model (c). We can see that the smoothing distorted model exhibits larger structure distortion than the noise distorted model, since the edges in (c) are severely blurred. We compute the roughness similarity and the structure similarity between the distorted model and the reference model, and the results are shown in Table II. In the roughness comparison, the similarity of the noise distorted model (b) is similar to that of the smoothing distorted model (c). While in the structure comparison, the similarity of the noise distorted model (b) is larger than that of the smoothing distorted model (c). This example shows that the proposed computation of structure similarity is able to measure the distortion imposed on the structure information of 3D meshes better than the roughness similarity.

In the proposed method, a final quality score is computed from the structure similarity value S_S and the perceptual

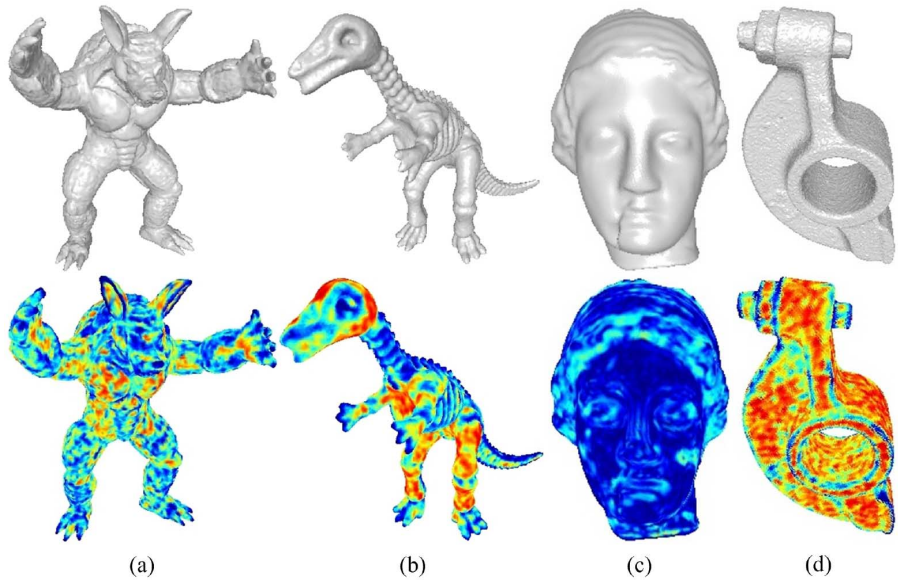

Fig. 9. Roughness distortion maps. (a) Armadillo (b) Dyno. (c) Venus. (d) RockerArm. Warmer colors represent higher values.

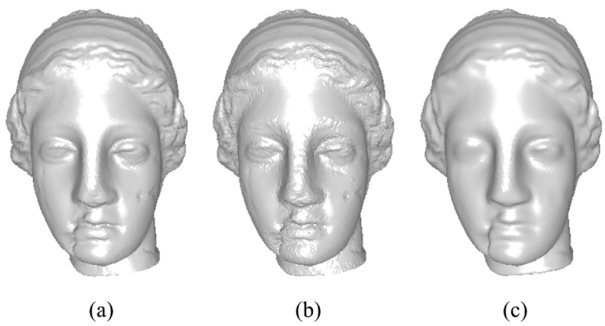

Fig. 10. Noise distorted and smoothing distorted models of the Venus. (a) Original Venus model. (b) A distorted model created by adding random noise. (c) A distorted model created by applying Taubin smoothing with step number at 20.

TABLE II
ROUGHNESS SIMILARITY AND STRUCTURE SIMILARITY BETWEEN TWO DISTORTED MODELS AND THE REFERENCE MODEL

	Mesh in Fig. 10(b)	Mesh in Fig. 10(c)
Roughness Similarity	0.865	0.860
Structure Similarity	0.938	0.746

roughness similarity value S_R by using the pooling function as follows:

$$S_{\text{pool}}(M^r, M^d) = (1-\alpha)\cdot S_R(M^r, M^d) + \alpha \cdot S_S(M^r, M^d) \tag{8}$$

where α is a weighting parameter. A smaller α gives more emphasis on the roughness distortion.

IV. EXPERIMENTAL RESULTS

In this section, we evaluate the performance of the proposed quality assessment method on three publicly available databases: the LIRIS/EPFL general-purpose database [1], the LIRIS masking database [12], and the UWB compression database [8]. We determine the parameters of the proposed method by one database, and use the same parameters in the other two databases for validation. We rotate this parameter determination and validation process for different databases; i.e. using the LIRIS/EPFL general-purpose database for parameter determination and the other two databases for validation; then using the LIRIS masking database and the UWB compression database for parameter determination. The performance of the proposed method is measured by computing the average performance from using these three sets of parameters. We compare the performance of the proposed method with relevant existing quality assessment methods including the state-of-the-art ones, in terms of accuracy and robustness. These methods include the Hausdorff distance (HD), RMS (root mean square error), GL1 [6], GL2 [22], SF [7], 3DWPM1 [23], 3DWPM2 [23], MSDM [1], MSDM2 [2], FMPD [3], DAME [8], and TPDM [5].

A. Databases

Here we give a brief introduction of the three databases used in the experiments. The LIRIS/EPFL general-purpose database [1] includes 4 reference models, and 84 distorted models (21 distorted models for each reference model). Two types of distortions are included in the database: random noise and smoothing distortion, to simulate various artifacts from geometry processing operations, such as compression and simplification. A score between 0 (best) and 10 (worst) is given to each distorted model by observers, and a normalized MOS is computed for each model by averaging the scores given by observers. The LIRIS masking database [12] includes 4 reference models, and 24 distorted models (6 distorted models for each reference model). The distorted models in the database are created by adding random noise with different strength in rough or smooth regions of the reference models. The database is built to test the visual masking effect in quality assessment of 3D meshes. A normalized score between 0 (worst) and 4 (best) is assigned to each distorted model. The UWB compression database [8] includes 5 reference models, and 63 distorted models (12 or

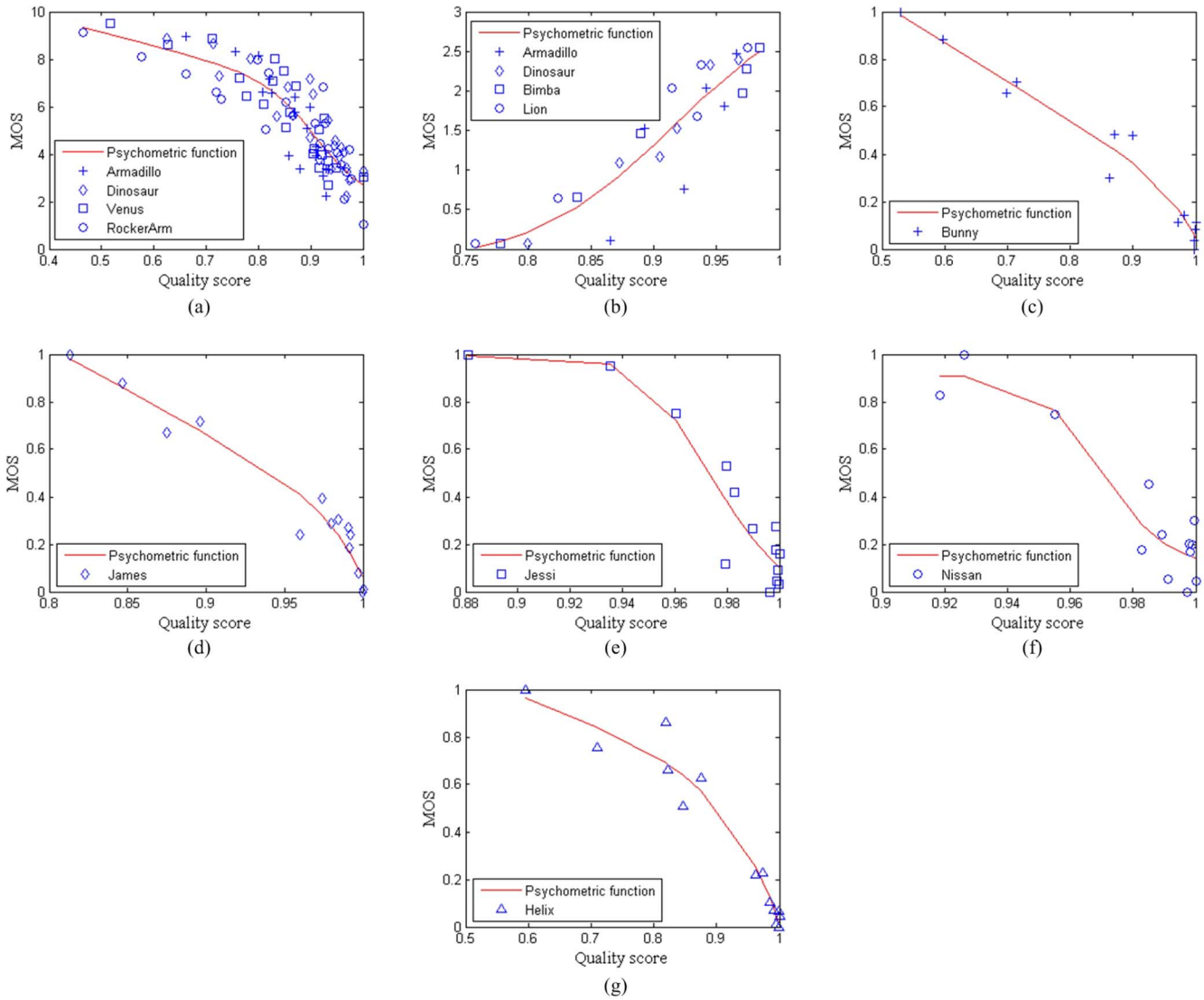

Fig. 11. Scatter plots of MOSs versus the predicted scores from the proposed model for the meshes in the three databases. (a) LIRIS/EPFL general-purpose database. (b) LIRIS masking database. (c) Bunny model. (d) James model. (e) Jessi model. (f) Nissan model. (g) Helix model in the UWB compression database.

13 distorted models for each reference model). Thirteen types of artificial distortions related with compression are applied on the reference models. Observers sorted the distorted models of each reference model according to the perceived quality, and a score between 0 (reference level) and 1 (worst) is computed based on the sorting results. Note that there is no correlation between the scores given to distorted models corresponding to different reference models, due to the procedure of the subjective tests. For example, a distorted model of Bunny with score "1" does not have similar visual quality as a distorted model of Jessi with score "1". Therefore, the performance of all the test methods on the UWB Compression Database is derived by averaging the performance on the 5 model sets.

B. Accuracy and Robustness Evaluation

Fig. 11 illustrates the scatter plots of the proposed quality assessment method on these three databases. The parameters used in the experiments are determined by the LIRIS/EPFL general-purpose database, and the parameters are set as $\sigma_o = 40$, $\omega_r = 1$, $\omega_e = 1.2$, $\beta = 0.5$, and $\alpha = 0.1$. The psychometric function in each plot maps the computed quality scores to the MOSs. It has been employed by existing quality assessment methods [5], [20], [32] to remove any nonlinearity from the subjective viewing tests. We employed the following function:

$$f(S) = \nu_1 \cdot \left(\frac{1}{2} - \frac{1}{1+\exp(\nu_2 \cdot (S - \nu_3))}\right) + \nu_4 \cdot S + \nu_5 \tag{9}$$

where $\nu_1, \nu_2, \nu_3, \nu_4$, and ν_5 are parameters to be fitted by minimizing the sum of squared differences between the mapped quality score and the MOSs. As can be observed from the scatter plots, the proposed method performs well on these three databases. The computed quality scores exhibit the similar distributions as the MOSs in most cases.

To compare the performance of the quality assessment methods with other related ones, two measures are used in this study. The Pearson linear correlation coefficient (r_p) is employed to measure the prediction accuracy, and the Spearman

TABLE III
CORRELATION COEFFICIENTS SPEARMAN r_s AND PEARSON r_p (%) OF THE PROPOSED OBJECTIVE METRIC ON TEST DATABASES

	General Purpose		Masking		Compression	
	Spearman(r_s)	Pearson(r_p)	Spearman(r_s)	Pearson(r_p)	Spearman(r_s)	Pearson(r_p)
Experiment 1	87.0	88.1	91.1	91.9	84.1	96.4
Experiment 2	86.4	87.5	93.3	93.0	84.2	96.2
Experiment 3	86.3	87.4	93.0	92.9	84.2	96.2
Average	86.6	87.7	92.5	92.6	84.2	96.3

TABLE IV
CORRELATION COEFFICIENTS SPEARMAN r_s AND PEARSON r_p (%) OF DIFFERENT OBJECTIVE METRICS ON TEST DATABASES

	General Purpose		Masking		Compression	
	Spearman(r_s)	Pearson(r_p)	Spearman(r_s)	Pearson(r_p)	Spearman(r_s)	Pearson(r_p)
Hausdorff	13.8	11.4	26.6	20.2	24.5	14
RMS	26.8	28.1	48.8	41.2	52	49
GL1	33.1	35.5	42	39.6	66.9	70.6
GL2	39.3	42.4	40.1	38.3	73.9	76.1
SF	15.7	7	38.6	15.5	57.4	34.8
3DWPM1	69.3	61.8	29.4	31.9	81.9	84.1
3DWPM2	49	49.6	37.4	42.7	80.9	82.3
MSDM	73.9	75	65.2	69.2	83.1	91.5
MSDM2	80.4	81.4	89.6	87.3	78	89.3
FMPD	81.9	83.5	80.2	80.8	81.8	88.8
DAME	76.6	75.2	68.1	58.6	**85.6**	**93.5**
TPDM	**89.6**	**86.2**	**90**	**88.6**	82.9	91.5
Proposed	**86.6**	**87.7**	**92.5**	**92.6**	**84.2**	**96.3**

TABLE V
CORRELATION COEFFICIENTS SPEARMAN r_s AND PEARSON r_p (%) OF DIFFERENT MODULES ON TEST DATABASES

	General Purpose		Masking		Compression	
	Spearman	Pearson	Spearman	Pearson	Spearman	Pearson
Roughness Difference Alone without Modulation	78.2	81.3	60.7	65.8	83.0	95.7
Roughness Difference Alone with Modulation	86.6	87.7	92.0	92.3	84.2	96.2
Structure Distortion Alone	26.0	26.3	13.8	5.2	80.5	93.0
Modulated Roughness Difference + Structure Distortion	87.0	88.1	91.1	91.9	84.1	96.4

rank-order correlation coefficient (r_s) is employed to measure the prediction monotonicity. The Spearman rank-order correlation coefficient depends only on the rank of the objective scores of the models; if the rank of objective scores is similar as the rank of MOSs, a high value will be obtained, regardless of the distance between the objective score and the corresponding MOS. For both the criteria, a higher value indicates better prediction performance.

Table III shows the values of r_s and r_p from the proposed metric on the three databases by using three different sets of parameters. In Experiment 1, The parameters are obtained from the LIRIS/EPFL general-purpose database; in Experiment 2, the parameters are obtained from the LIRIS masking database; in Experiment 3, the parameters are obtained from the UWB compression database. Note that there are two performance measures, r_s and r_p, and we determine the parameters by maximizing the r_s values in the experiments. The performance of the proposed method is measured by computing the average r_s and r_p values.

The values of r_s and r_p from the test metrics on the three databases are listed in Table IV, where the two highest correlation coefficients have been highlighted in boldface. The proposed method has the highest r_s and r_p values on the LIRIS masking database (Masking). The LIRIS masking database is designed to evaluate the visual masking effect in quality assessment of 3D meshes. The good performance of the proposed method in the database confirms the effectiveness of the proposed visual masking module in this work. The proposed method has comparable performance to TPDM [5] on the LIRIS/EPFL general-purpose database (General Purpose), and to DAME [8] on the UWB compression database (Compression).

The TPDM [5] performs the best or close to the best on the LIRIS/EPFL general-purpose database and the LIRIS masking database, but is slightly worse than the best two methods on the UWB compression database. The DAME [8] has the highest r_s value on the UWB compression database, but it is poor on the LIRIS/EPFL general-purpose database and the LIRIS masking database. Overall, the proposed method gives more consistent performance across the three databases.

Table V shows the values of r_s and r_p from the proposed metric on the three databases by using the roughness difference alone (with/without the masking and saturation modulation), the structure distortion alone, and the modulated roughness difference together with the structure distortion. The parameters used in the experiments are determined by the LIRIS/EPFL

general-purpose database, the same as the parameters used in Fig. 11.

Table V shows that the roughness difference exhibits high correlation with the MOSs, and by integrating the masking and saturation modules, the correlation between the roughness difference and the MOSs increases. We also find that the structure distortion alone does not correlate well with the MOSs in the databases. The reasons include two aspects. First, we use a simple formulation of the structure distortion in the proposed method. The proposed method computes the structure distortion by detecting strong edges and computing the similarity of the edge strength between the distorted and reference meshes, and this formulation may not be able to measure the structure distortion accurately. Second, the structure distortion is not the major distortion occurring on the meshes of the test databases. On the LIRIS masking database, random noise is added to smooth or rough regions of the 3D meshes, and the structure information is not severely degraded. Thus, the structure distortion can not measure the quality of these noise-distorted meshes. Further, the combination of the structure distortion and the roughness difference does not exhibit higher correlation with the MOSs than the roughness difference alone. On the LIRIS/EPFL general-purpose and the UWB compression databases, the types of distortion include mesh smoothing and compression, and these types of distortion mainly degrade the structure information of 3D meshes. Thus, the structure distortion yields better performance on the LIRIS/EPFL general-purpose and the UWB compression databases. The combination of the structure distortion and the roughness difference also gives slightly better performance than the roughness difference alone on these two database. In summary, the proposed masking and saturation modulation is able to improve the performance of the roughness difference. Besides, it is possible to improve the performance of the quality metric by integrating the structure distortion with the roughness difference, but to achieve this goal, a more accurate formulation of the structure distortion needs to be designed in the future work.

V. Conclusion

We have designed and implemented a new method to assess the perceptual quality of 3D triangle meshes. Given a distorted 3D model and a reference one, we compute a roughness measure by using mean curvature and compare the roughness difference between each pair of corresponding vertices. The roughness variation is modulated with a visual masking module and a saturation module. With the visual masking module, computed distortion in rough vertices are masked. With the saturation module, high-level roughness distortion decreases to account for the decrease in sensitivity of the HVS at high distortion levels. The structure similarity between two models is computed based on the maximum curvature between edge vertices of the two models. A quality score is derived as the integration of the perceptually modulated roughness distortion and the structure similarity. Compared with relevant existing quality assessment methods for 3D triangle meshes, the proposed method yields more consistent results with subjective scores on three publicly available databases.

The limitation of the current stage of development for the proposed method is that it is only used for geometrical processing that preserves mesh connectivity. Extending the proposed method to distortions which affect the vertex connectivity, such as model simplification, will be a possible direction of future work. Another possible extension is to combine visual attention in quality metrics for 3D meshes, and further psychophysical experiments are needed before we integrate visual attention into a quality metric.

References

[1] G. Lavoué, E. D. Gelasca, F. Dupont, A. Baskurt, and T. Ebrahimi, "Perceptually driven 3D distance metrics with application to watermarking," in *Proc. SPIE*, 2006, Art. ID 63120L.

[2] G. Lavoué, "A multiscale metric for 3D mesh visual quality assessment," *Comput. Graph. Forum*, vol. 30, no. 5, pp. 1427–1437, 2011.

[3] K. Wang, F. Torkhani, and A. Montanvert, "Technical section: A fast roughness-based approach to the assessment of 3D mesh visual quality," *Comput. Graph.*, vol. 36, no. 7, pp. 808–818, Nov. 2012.

[4] F. Torkhani, K. Wang, and J.-M. Chassery, "A curvature tensor distance for mesh visual quality assessment," in *Computer Vision and Graphics*, ser. Lecture Notes in Comput. Sci., L. Bolc, R. Tadeusiewicz, L. Chmielewski, and K. Wojciechowski, Eds. Berlin, Germany: Springer-Verlag, 2012, vol. 7594, pp. 253–263.

[5] F. Torkhani, K. Wang, and J.-M. Chassery, "A curvature-tensor-based perceptual quality metric for 3D triangular meshes," *Mach. Graph. Vis.*, to be published.

[6] Z. Karni and C. Gotsman, "Spectral compression of mesh geometry," in *Proc. 27th Annu. Conf. Comput. Graph. Interactive Techniques*, 2000, pp. 279–286.

[7] Z. Bian, S.-M. Hu, and R. R. Martin, "Evaluation for small visual difference between conforming meshes on strain field," *J. Comput. Sci. Technol.*, vol. 24, no. 1, pp. 65–75, 2009.

[8] L. Váša and J. Rus, "Dihedral angle mesh error: A fast perception correlated distortion measure for fixed connectivity triangle meshes," *Comput. Graph. Forum*, vol. 31, no. 5, pp. 1715–1724, 2012.

[9] W. Lin and C.-C. Jay Kuo, "Perceptual visual quality metrics: A survey," *J. Vis. Commun. Image Representation*, vol. 22, no. 4, pp. 297–312, 2011.

[10] W. Lin, T. Ebrahimi, P. C. Loizou, S. Möller, and A. R. Reibman, "Introduction to the special on new subjective and objective methodologies for audio and visual signal processing," *IEEE J. Sel. Topics Signal Process.*, vol. 6, no. 6, pp. 614–615, Oct. 2012.

[11] I. Cheng and A. Basu, "Perceptually optimized 3-D transmission over wireless networks," *IEEE Trans. Multimedia*, vol. 9, no. 2, pp. 386–396, Feb. 2007.

[12] G. Lavoué, "A local roughness measure for 3D meshes and its application to visual masking," *ACM Trans. Appl. Perception*, vol. 5, no. 4, pp. 21:1–21:23, 2009.

[13] L. Qu and G. W. Meyer, "Perceptually guided polygon reduction," *IEEE Trans. Vis. Comput. Graphics*, vol. 14, no. 5, pp. 1015–1029, Sep.–Oct. 2008.

[14] S. Hillaire *et al.*, "Design and application of real-time visual attention model for the exploration of 3D virtual environments," *IEEE Trans. Vis. Comput. Graph.*, vol. 18, no. 3, pp. 356–368, Mar. 2012.

[15] L. Dong, W. Lin, Y. Fang, S. Wu, and H. S. Seah, "Saliency detection in computer rendered images based on object-level contrast," *J. Vis. Commun. Image Representation*, vol. 25, no. 3, pp. 525–533, 2014.

[16] S. Daly, *Digital Images and Human Vision*. Cambridge, MA, USA: MIT Press, 1993.

[17] C. J. Van den Branden Lambrecht and O. Verscheure, "Perceptual quality measure using a spatiotemporal model of the human visual system," in *Proc. SPIE*, 1996, pp. 450–461.

[18] A. Ninassi, O. Le Meur, P. Le Callet, and D. Barba, "Considering temporal variations of spatial visual distortions in video quality assessment," *IEEE J. Sel. Topics Signal Process.*, vol. 3, no. 2, pp. 253–265, Apr. 2009.

[19] Y. Zhao, L. Yu, Z. Chen, and C. Zhu, "Video quality assessment based on measuring perceptual noise from spatial and temporal perspectives," *IEEE Trans. Circuits Syst. Video Technol.*, vol. 21, no. 12, pp. 1890–1902, Dec. 2011.

[20] A. Liu, W. Lin, and M. Narwaria, "Image quality assessment based on gradient similarity," *IEEE Trans. Image Process.*, vol. 21, no. 4, pp. 1500–1512, Apr. 2012.

[21] Z. Wang, A. C. Bovik, H. R. Sheikh, and E. P. Simoncelli, "Image quality assessment: From error visibility to structural similarity," *IEEE Trans. Image Process.*, vol. 13, no. 4, pp. 600–612, Apr. 2004.
[22] O. Sorkine, D. Cohen-Or, and S. Toledo, "High-pass quantization for mesh encoding," in *Proc. 2003 Eurograph./ACM SIGGRAPH Symp. Geometry Process.*, 2003, pp. 42–51.
[23] M. Corsini, E. Gelasca, T. Ebrahimi, and M. Barni, "Watermarked 3-D mesh quality assessment," *IEEE Trans. Multimedia*, vol. 9, no. 2, pp. 247–256, Feb. 2007.
[24] G. Lavoué and M. Corsini, "A comparison of perceptually-based metrics for objective evaluation of geometry processing," *IEEE Trans. Multimedia*, vol. 12, no. 7, pp. 636–649, Nov. 2010.
[25] M. Corsini *et al.*, "Perceptual metrics for static and dynamic triangle meshes," *Comput. Graph. Forum*, vol. 32, no. 1, pp. 101–125, 2013.
[26] S.-J. Kim, S.-K. Kim, and C.-H. Kim, "Discrete differential error metric for surface simplification," in *Proc. 10th Pacific Conf. Comput. Graph. Appl.*, Oct. 2002, pp. 276–283.
[27] M. Desbrun, M. Meyer, and P. Alliez, "Intrinsic parameterizations of surface meshes," *Comput. Graph. Forum*, vol. 21, no. 3, pp. 209–218, 2002.
[28] P. Alliez, D. Cohen-Steiner, O. Devillers, B. Lévy, and M. Desbrun, "Anisotropic polygonal remeshing," *ACM Trans. Graph.*, vol. 22, no. 3, pp. 485–493, 2003.
[29] M. P. Eckert and A. P. Bradley, "Perceptual quality metrics applied to still image compression," *Signal Process.*, vol. 70, no. 3, pp. 177–200, 1998.
[30] A. B. Watson, R. Borthwick, and M. Taylor, "Image quality and entropy masking," *Human Vis., Visual Process., Digital Display VIII*, vol. 3016, pp. 2–12, 1997.
[31] A. Ninassi, O. Le Meur, P. Le Callet, and D. Barba, "Considering temporal variations of spatial visual distortions in video quality assessment," *IEEE J. Sel. Topics Signal Process.*, vol. 3, no. 2, pp. 253–265, Apr. 2009.
[32] J. Wu, W. Lin, G. Shi, and A. Liu, "Perceptual quality metric with internal generative mechanism," *IEEE Trans. Image Process.*, vol. 22, no. 1, pp. 43–54, Jan. 2013.

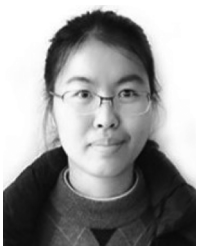

Lu Dong received the B.S. degree from Suzhou University, Suzhou, China, in 2009, and is working toward the Ph.D. degree in computer engineering at Nanyang Technological University, Singapore.

In 2015, she joined the Minieye Research and Development Center, Nanjing, China. Her research interests include perceptual computer graphics and image rendering.

Yuming Fang received the B.E degree from Sichuan University, Chengdu, China, in 2006, the M.S. degree from the Beijing University of Technology, Beijing, China, in 2009, and the Ph.D. degree in computer engineering from Nanyang Technological University, Singapore, in 2013.

He is currently an Associate Professor in the School of Information Technology, Jiangxi University of Finance and Economics, Nanchang, China. He was previously a (Visiting) Postdoc Research Fellow with the following institutions: IRCCyN Laboratory, PolyTech' Nantes, University of Nantes, Nantes, France; the University of Waterloo, Waterloo, ON, Canada; and Nanyang Technological University, Singapore. His research interests include visual attention modeling, visual quality assessment, image retargeting, computer vision, and 3D image/video processing.

Prof. Fang was a Secretary of the 9th Joint Conference on Harmonious Human Machine Environment (HHME 2013). He was also a Special Session Organizer for VCIP 2013 and QoMEX 2014.

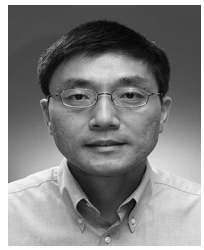

Weisi Lin (S'91–M'92–SM'00) received the Ph.D. degree from King's College, London University, London, U.K., in 1993.

He served as the Laboratory Head of Visual Processing, Institute for Infocomm Research, Singapore. Currently, he is an Associate Professor with the School of Computer Engineering, Institute for Infocomm Research. He has authored or coauthored over 130 journal papers and 200 conference papers, as well as authored 2 books. He has filed 7 patents. His research interests include image processing, perceptual signal modeling, video compression, and multimedia communication.

Prof. Lin is currently an Associate Editor for the IEEE TRANSACTIONS ON IMAGE PROCESSING, IEEE SIGNAL PROCESSING LETTERS, and the *Journal of Visual Communication and Image Representation*, and was previously an Associate Editor for the IEEE TRANSACTIONS ON MULTIMEDIA. He has also served as a Guest Editor for eight special issues in international journals. He has been a Technical Program Chair for IEEE ICME 2013, PCM 2012, and QoMEX 2014. He has been an Invited/Panelist/Keynote/Tutorial Speaker in over ten international conferences, as well as a Distinguished Lecturer of the Asia-Pacific Signal and Information Processing Association (APSIPA), 2012–2013.

Hock Soon Seah received the B.E. degree in electrical engineering from the National University of Singapore, Singapore, in 1983, the M.S. degree in computing science from the University of London, London, U.K., in 1988, and the Ph.D. degree in computer graphics from the Nanyange Technological University, Singapore, in 2000.

He is currently a Professor with the School of Computer Engineering, Nanyang Technological University (NTU), Singapore. He is also Director of the Multi-plAtform Game Innovation Centre (MAGIC), NTU, which is supported by the Singapore National Research Foundation.

Prof. Seah is a Fellow of the Singapore Academy of Engineering.